Astronomy with Millimeter and Submillimeter Wave Interferometry
ASP Conference Series, Vol. 59, 1994
M. Ishiguro and Wm. J. Welch (eds.)

THE IRAM INTERFEROMETER ON PLATEAU DE BURE

S. GUILLOTEAU
Institut de Radioastronomie Millimétrique (IRAM), 300 Rue de la Piscine, 38406 Saint Martin d'Hères, France

ABSTRACT In November 1992, the IRAM interferometer on Plateau de Bure has reach two years of operation. After a review of its current technical status, with emphasis on its specificities, this paper presents an overview of its capabilities, illustrated by examples taken from the scientific program carried on during these two years. On-going upgrades and future plans are presented.

INTRODUCTION

Millimeter wave interferometers are unique tools to study dust and molecular gas in outflows from protostars, circumstellar envelopes around evolved stars, dense cores of molecular clouds in our Galaxy, as well as the distribution of molecular gas in other galaxies. Since all of these objects are cool, typically 10–500 K, observations are limited by sensitivity. Signal-to-noise ratios larger than about one hundred are exceptional. The IRAM interferometer was originally designed with these constraints, which lead to the choice of relatively large antennas to maximize the sensitivity.

The original instrument is described in detail by Guilloteau *et al.* (1992). This paper presents an update of the status of the interferometer and illustrates its capacities.

THE INSTRUMENT

Array and Site

The IRAM interferometer on Plateau de Bure consists of three 15 m diameter antennas. These can be placed on 26 stations arrayed along a T shaped rail track that extends 160 m north-south and 288 m east-west.

Contrary to all other mm-interferometers wich are located in valleys at altitudes about 1300 m, it is located on the top of a mountain, the Plateau de Bure, which was selected because of its altitude (2550 m) and flatness: baselines as long as 1.5 km can be constructed. The altitude helps providing excellent atmospheric transparencies: in winter, the precipitable water vapor is often less than 2 mm. However, these conditions are obtained at the expense of some severe constraints: temperatures may go down to −30° C, heavy snowfalls and icing conditions are not exceptional. Moreover, there is no road to the Plateau so all personnel and material are transported to the site by cable car (*téléphérique*).

The array phase center is 5°54′28.5″ E longitude and 44°38′2.0″ N latitude and at the antennas' Cassegrain foci, 8 m above the tracks, the altitude is 2560 m.

Antennas

The 15-m dishes (Delannoy 1985, 1991) are made largely of carbon fiber, which allows the antenna to preserve its surface accuracy without any thermal control. The current surface accuracy of the antennas, measured by holography, is about 70μm. No attempt to improve this figure was made, since the antennas are essentially perfect at 3 mm. Because of the shiny mirror surface, the antennas must not be pointed within 35° of the Sun.

Homologous deformations of the telescope structure and mount imperfections are compensated with a trigonometric pointing model. Since most of the model parameters are telescope constants, however, and the station inclination is measured with an inclinometer, only the azimuth encoder zero must in principle be redetermined when an antenna is moved. The nominal pointing accuracy, $< 4''$ r. m. s., is regularly achieved during radio pointing sessions that accompany each array reconfiguration. The 3-years experience with the array show that the pointing accuracy is limited by small thermal drifts (up to 5″) affecting the mount inclination and the encoder zeros. Since only one astronomical sources is required to redetermine the whole pointing model, theses drifts can be compensated by regular (every few hours) cross scan measurements on a strong source.

Receivers

The IRAM interferometer is now equipped with SIS receivers tunable from 80–115 GHz. Each receiver is equipped by a single phase locked Gunn diode oscillators, operating in the same 80-115 GHz band, to generate the local oscillator (LO_1) signals, which are injected into the corrugated scalar feed horns through a quasi-optic diplexer. The LO_1 is derived through an harmonic mixer from another oscillator (LO_2) around 1.85 GHz, which is also used to down-convert the first intermediate frequency, $IF_1 = 1.5$ GHz, to the 100-650 MHz band transmitted through cables to the central building. Cooled HEMT amplifiers at used at the first IF. With such a frequency scheme, the effective IF_1 is slightly variable.

The receivers have instantaneous bandwidths of 500 MHz and can be operated in DSB mode, or tuned to reject the USB by 3–6 dB. DSB receiver temperatures at 90 GHz are 40-50 K, and SSB system temperatures, including atmospheric losses, can be as low as 150 K. For calibration, an ambient temperature absorber is slid in front of the horn.

Receivers are tuned remotely by the control computer. A semi-automatic tuning program is available to preset the receiver at known frequencies.

Correlators

Until Aug-1992, two digital complex cross-correlators were used simultaneously: a wide band, *continuum* correlator and a narrow band, *spectral* correlator.

These correlators have now been replaced by a new flexible spectral correlator system. This correlator is made of 6 fully independent units. Each units processes 6 baselines and 4 antennas. The multiplier boards, based on the NFRA correlator chip (Bos 1986), achieve 88% efficiency with four level

https://doi.org/10.1017/S0252921100019047 Published online by Cambridge University Press

sampling. Digital delays are used. Data acquisition and correlator control are done by a Motorola 68030 microprocessor connected to the central computer by Ethernet.

Each unit can operate in 4 modes (see table), and is tunable anywhere in the IF band by steps of 0.625 MHz. Because of channel shape and apodization the

Mode	Bandwidth (MHz)	Number of channels	Channel Width (MHz)
1	160	64	2.5
2	80	128	0.625
3	40	256	0.156
4	20	256	0.078

effective resolution is about 1.6 times broader than the nominal channel spacing and the noise bandwidth is 1.87 times the channel spacing. A non-apodized mode with slightly higher resolution is available for special experiments. As in the previous correlators, all delays are fully digital, obtained by shift memories operating at the sampling speed of 160 MHz.

All units are plugged in a general IF distribution system which can connect any unit to one of the two available IF cables, or to a common noise source for calibration of their frequency dependent phase responses. This scheme provides very accurate (better than 1 degree) channel per channel phase calibration. Amplitude response calibration is obtained by normalizing the cross-correlation by the square root of the auto-correlation products.

The basic integration cycle is 1 second, the cycle time of the Walsh functions which are used to modulate the LO_1 phase to reduce cross-talk and allow sideband separation. The microprocessor applies all the necessary real-time processing to the raw data to provide time averaged results to the host computer. This include correlator chip reading, Walsh demodulation, sideband separation, clipping corrections, apodization, Fourier transform, small delay offsets (since the delay step is 6.25 nsec) and phase bandpass corrections every second, and accumulation in an integration buffer. The final integration time ranges from 4 seconds to 4 minutes, depending on the observing procedure.

The correlator units also provide a frequency averaged information (complex visibility) every second to the host computer for monitoring. This particularity allows nearly instantaneous display of the fringe amplitude and phase on strong lines or continuum sources.

Control System

The IRAM interferometer is controlled by a central Digital VAX 3400 computer linked to several embedded microprocessors through a CAMAC interface. A second VAX, which shares disk space with the control computer, is used for almost real-time and off-line data reduction.

The user interface program, OBS (Guilloteau 1990), is similar to the one used at the IRAM 30 m telescope. It is based on a command interpreter that allows flexible programming with parametrized observing procedures. There are commands for instrument setup, IF bandpass and atmospheric transmission calibration, and receiver gain ratio, delay offset, pointing, and focus measurements. Standard procedures are used for most observations, including pointing sessions, baseline determination, image synthesis, and even series of snapshots. In addition to the high level interface, individual parts of the system can be controlled independently from a menu. An alarm notifies the array operator of any anomalies, including the end of an observing procedure.

Atmospheric amplitude calibrations (opacity corrections and auto-correlation normalization) are automatically applied to the data by the on-line computer, and written on disk. This data is archived daily on Exabyte cassettes.

A dedicated program, CLIC (Lucas 1991), was developed for reducing interferometer data. Its basic facilities include data display, editing, time averaging, and atmospheric opacity calibration. Observations of reference sources are used to calibrate the RF bandpass, the flux scale, and the source amplitude and phase. Calibrated visibilities are then tabulated for further processing (mapping). There are also several specialized routines for interferometer setup, including reduction of interferometric pointing and focus measurements, and determination of the interferometer baseline lengths from observations of point sources with known positions.

Data Processing

The CLIC program is the main tool to calibrate the interferometer data. After this step, maps can be made and processed interactively with the GILDAS (Guilloteau & Forveille 1989) image processing system. Available tasks allow map construction from *uv* data, and CLEANing maps with any of several variants of the basic algorithm. Direct analysis from *uv* plane visibility data, such as determination of source positions, flux densities and sizes, are also possible. Mosaic construction and deconvolution can be performed with a modified CLEAN program, and single dish data can be merged with interferometer data to provide short spacing information. Data also can be translated into UVFITS or FITS formats for transport to other image processing software.

Operation

Another peculiarity of the IRAM interferometer is to be operated as a full service instrument by the IRAM staff. The array is reconfigured roughly every two or three weeks, with typically ten projects observed in parallel. Moving all three antennas requires 2 to eight hours (essentially depending on snow amounts), and 3 more hours are required for the subsequent pointing, delay, and baseline measurements.

PERFORMANCE AND CAPABILITIES

The peculiarity of the IRAM interferometer is its large dishes. This results in high sensitivity, but limited field of view. The antenna beam FWHM is 55″ at 90 GHz. It is possible to image a wider field of view by mosaicing. The shortest possible spacing is 24 m so even though projection shortens the effective baselines, structures larger than about 30″ are heavily resolved. Two standard configuration sets are available: a compact one (3.5″ at 90 GHz), and one for high resolution (about 2″ at 110 GHz).

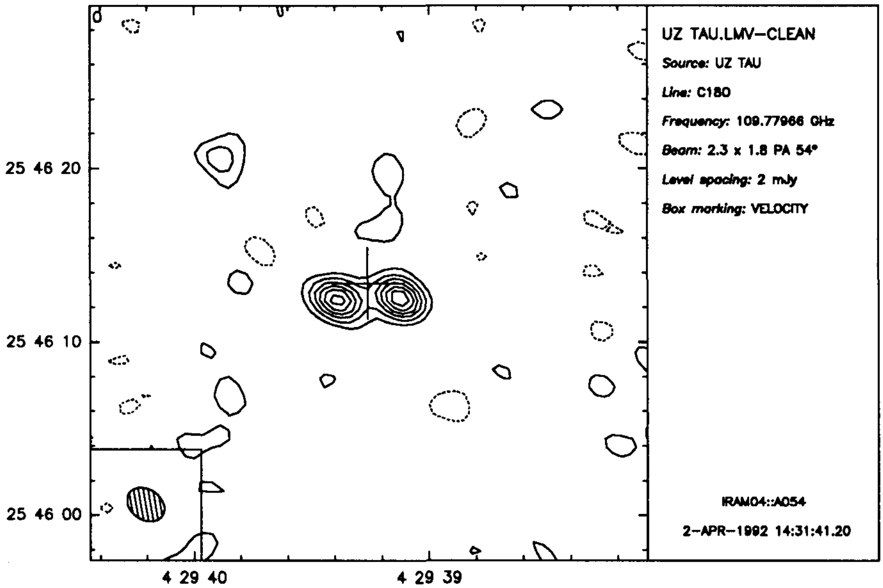

FIGURE I Continuum emission from the triple star UZ Tau (from Simon and Guilloteau 1992).

Sensitivity

The continuum sensitivity is typically δS = 1.7–2.8 mJy in a one hour DSB integration at 90 GHz. For a full synthesis with 36 h integration on source, this goes down to about 0.4 mJy. For spectral lines, with 625 kHz channel spacing and 36 h integration on source, the typical r.m.s. noise δT_b = 0.14 K for the "compact" array, and $\simeq$ 0.4 K for the high resolution array. At 115 GHz, the sensitivity degrades by a factor 2-3 because of higher atmospheric opacities and receiver noise (SSB tuning is not possible at this frequency).

Angular Resolution

The primary use of sensitivity is high angular resolution. The IRAM interferometer can provide better 2″ resolution at 110 GHz. A good illustration of both sensitivity and resolution is given in Fig 1, which shows a continuum map of the triple star UZ Tau (from Simon and Guilloteau, 1992) with 2.3 × 1.8″ resolution and 1 mJy rms noise. Yet, this map was obtained with only 6 hours of observing time.

Because of this sensitivity, the IRAM interferometer has provided the first very high resolution ($\simeq$ 2″) images of molecular species like HCN and HCO^+ in nearby galaxies such as IC342 (Downes et al., 1992, Rieu et al., this issue), enabling for the first time comparison between the distribution of dense gas and more diffuse molecular gas traced by CO on the giant molecular cloud scale. The broad bandwidth of the new correlator system will allow such studies in many more galaxies.

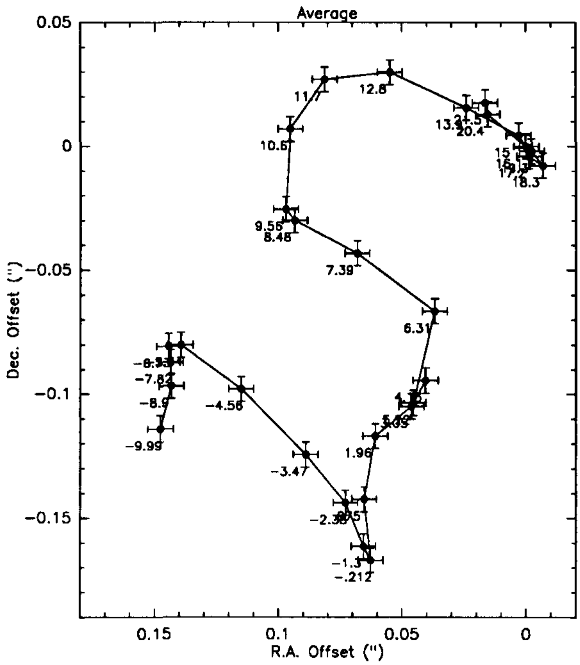

FIGURE II Relative positions of the SiO J=2-1 masers in Orion A IRC-2

The interferometer has also been used in "snapshot" mode (2 or 3 one hour integrations for each source per configuration, with a total of 6 to 12 baselines) to study a large number of circumstellar envelopes in CO and SiO (Lucas et al. 1992). This mode is specially suited when the size and strength of the source are the most important parameters to measure. An overview of the observations performed on circumstellar envelopes with the IRAM interferometer are presented in this issue by R. Lucas.

Calibration Accuracy

The high sensitivity also improves the calibration accuracy since point sources as weak as 0.5 Jy can be used as phase calibrators. Since more sources can be used, they can be chosen closer to the program objects. Phase errors introduced by baseline errors or atmospheric inhomogeneities are thereby reduced and the dynamic range and absolute positioning of the map improved. A "self-calibration" technique made possible by this high sensitivity was used for the HCN J=1-0 observations of the molecular outflow in the proto-planetary nebula CRL 618, resulting in a dynamic range of 50:1. (Neri et al. 1992).

The built-in calibration noise source also helps in obtaining high spectral dynamic range. This feature was used to map the SiO($2 \rightarrow 1$) masers in Ori A (IRC 2). The relative positions of the maser components have a positional accuracy better than 0.005″, even in the center of the double peaked line profile (Fig. 2). This is three times better than previous measurements (Plambeck et al. 1990) made with the interferometer at Hat Creek, California.

Along the same line is the detection of the CO J=1-0 line in absorption in

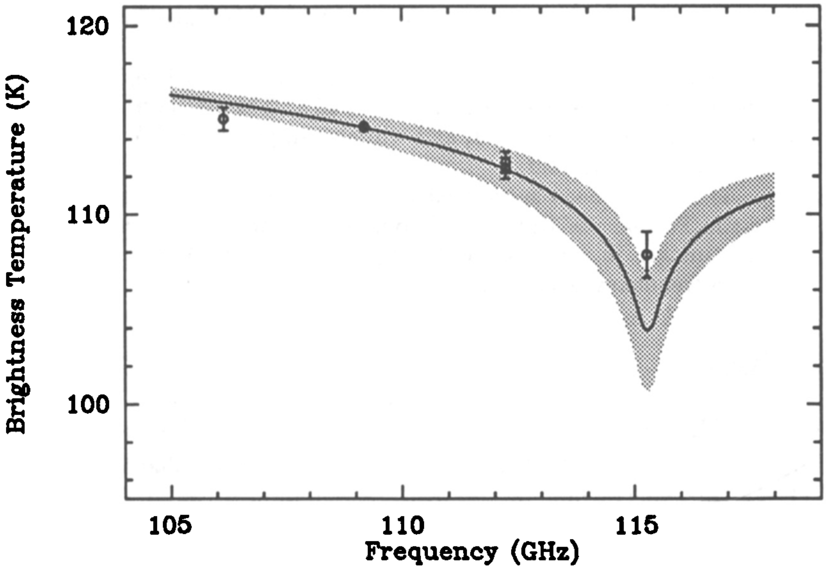

FIGURE III CO J=1-0 line in absorption in the troposphere of Neptune. The shaded area represents model profile computed for ±30% abundance variations around a CO mole fraction of $1.2 10^{-6}$. Errorbars (1 σ) include thermal noise and all instrumental effects.

the troposphere of Neptune (Fig. 3, from Guilloteau et al., 1993).

This detection, which definitely proves that CO originates from the planet interior, required a relative amplitude calibration of the two sidebands better than 0.5 %, achieved by frequent and sensitive observations of Uranus.

FUTURE

Improvements now underway will alleviate some current limitations of the instrument: the imaging speed is slow because there are only three antennas, the baseline lengths are < 300 m, and only the 3 mm band can presently be observed.

A fourth antenna is currently under construction. The mount is completed, and the antenna will be incorporated in the array early 1993. We intend to use this 4th antenna not only to speed up most observations, but also to improve sensitivity for high resolution work. The correlator system includes provision for using closure relations on a short integration time (down to 1 second).

A new generation of four channel receivers is under design. These receivers will have 2 independently tunable SIS mixers on opposite polarisation in the 80-115 GHz band, and 2 in the 205-270 GHz band. The optics will allow simultaneous observations with any pair of mixers, and fast switching between one pair and another. A prototype is under test in the laboratory. These specifications were set as a reasonable compromise between optimum use of the array at 1.3 mm and simple design with reliable operation. Dual-frequency operation and fast switching are essential to control the pointing accuracy to the level required by the narrow field of view at 1.3 mm (22″). Installation on the site is foreseen in 1994.

It is also planned to extend the tracks by about 50% in length (adding 3 more stations denominated N30, W20, and W30). This extension will allow sub-arcsecond resolution at 230 GHz, and will also improve the UV coverage for moderate resolution experiments.

A proposal has also been submitted to the funding agencies to add 2 more antennas to the Plateau de Bure interferometer. With 6 antennas, the array could produce images in just one configuration, an essential feature for high resolution, high frequency observations.

REFERENCES

Bos, A. 1986, The NFRA Correlator Chip (NFRA-ITR-176: Dwingeloo)

Delannoy, J. 1985, in (Sub)Millimeter Astronomy, ed. P. A. Shaver & K. Kjär (ESO: Garching) p25

Delannoy, J. 1991, in Radio Interferometry: Theory, Techniques, and Applications, ed. T. J. Cornwell & R. A. Perley, (ASP, San Francisco) p15

Downes, D., Radford, S. J. E., Guilloteau, S., Guélin, M., Greve, A., & Morris, D. 1992, A&A, 262,

Guilloteau, S. 1990, OBS User's Guide (IRAM: Grenoble)

Guilloteau, S., Delannoy, J., Downes, D., Greve, A., Guélin, M., Lucas, R., Morris D., Radford, S.J.E., Wink, J., Cernicharo, J., Forveille, T., Garcia-Burillo, S., Neri, R., Blondel, J., Perrigouard, A., Plathner, D., Torres, M., 1992, A&A 262 624

Guilloteau, S., & Forveille, T., 1989, Grenoble Image and Line Data Analysis System (GILDAS; IRAM: Grenoble)

Guilloteau, S., Dutrey, A., Marten, A., & Gautier, D., 1993, A&A submitted

Lucas, R., 1992, Continuum and Line Interferometer Calibration (CLIC; IRAM: Grenoble)

Lucas, R., 1993, this volume

Lucas, R., Bujarrabal, V., Guilloteau, S., Bachiller, R., Baudry, A., Cernicharo, J., Delannoy, J., Forveille, T., Guélin, M., & Radford, S. J. E. 1992, A&A, 262, 491

Neri, R., Garcia-Burillo, S., Guélin, M., Cernicharo, J., Guilloteau, S., & Lucas, R., 1992, A&A, 262, 544

Plambeck, R.L., Wright, M.C.H., & Carlstrom, J.E., 1990, ApJ 348, L65

Rieu N.Q., Viallefond, F., Combes, F., Jackson, J., Lequeux, J., Radford, S.J.E., Bach. T., 1993, this volume

Simon, M., & Guilloteau, S., 1992, ApJ, 397, L47